PHILOSOPHICAL TRANSACTIONS OF THE ROYAL SOCIETY A MATHEMATICAL, PHYSICAL & ENGINEERING SCIENCES

Time-Resolved Fluorescence from Biological Systems: Tryptophan and Simple Peptides

G. S. Beddard, G. R. Fleming, George Porter and R. J. Robbins

Phil. Trans. R. Soc. Lond. A 1980 **298**, 321-334
doi: 10.1098/rsta.1980.0257

Phil. Trans. R. Soc. Lond. A **298**, 321–334 (1980)
Printed in Great Britain

Time-resolved fluorescence from biological systems: tryptophan and simple peptides

By G. S. Beddard, G. R. Fleming, Sir George Porter, F.R.S., and R. J. Robbins
Davy Faraday Laboratory of the Royal Institution, 21 Albemarle Street, London W1X 4BS, U.K.

Four methods of applying mode-locked lasers to time-resolved fluorescence measurements in the subnanosecond region are compared. When time resolution below 100 ps is not required, the most precise and sensitive method is single-photon counting, and the application of this method to studies of time-resolved fluorescence of tryptophan in simple peptides is described. The dependence of lifetimes on pH and temperature are interpreted in terms of quenching by intramolecular proton and electron transfers.

Comparison of techniques for time-resolved fluorescence

Time-resolved fluorescence is an increasingly valuable technique in biological studies and the accessible time range has been extended about a thousandfold by the use of mode-locked lasers. Four principal methods of utilization of these pulses have been used: (1) the optical Kerr shutter; (2) the electro-optic streak camera; (3) time-correlated single-photon counting; (4) fluorescence up-conversion. Generally, methods 1 and 2 are used with single pulses from mode-locked solid state lasers and methods 3 and 4 are used with continuously working mode-locked dye lasers. We have used methods 1, 2 and 3 in our laboratory and the relative advantages and disadvantages may be summarized as follows.

The optical Kerr shutter has good time resolution but low sensitivity and low precision. The time resolution is limited by three factors: the pulse duration, the Kerr relaxation time, and dispersion. The sensitivity is low (dynamic range about 10) because of background intensity, from fluorescence leaking through the crossed polarizers during the entire fluorescence decay. Precision is poor since multiple shots are required and the reproducibility of pulses from solid state mode-locked lasers is poor.

The streak camera, when operated at its fastest streak speed, has a resolution of *ca.* 2 ps, although this is greatly reduced at the streak speeds normally used to record weak fluorescence. Reproducibility is improved over that of the Kerr shutter since the entire decay curve is recorded in a single shot. Dynamic range is *ca.* 100 and, although the precision is less than that of the photon counting method, we have found the streak camera to be the most useful technique at present available for the study of fluorescence decays of less than 100 ps. Our Nd glass–streak camera system has been used extensively in studies of photosynthetic systems *in vivo* (Porter *et al.* 1978) and particularly in the study of energy transfer in the red alga *Porphyridium cruentum* (Searle *et al.* 1978).

Both the above single-shot methods require a high energy per pulse and this is often a disadvantage since it may introduce unwanted effects such as exciton–exciton interactions and stimulated emission. If the pulse energy is lowered, the precision of the measurements is

seriously impaired. The repetitively scanning synchroscan camera, in combination with a continuous wave (c.w.) mode-locked laser, may provide a solution to these problems.

The third technique, that of time-correlated single photon counting, provides another solution. Here the time resolution is limited by transit time variations in the photomultiplier and by walk in the constant fraction discriminator. With deconvolution, a time resolution of about 50 ps is possible and this should improve in the near future. There is an improvement by a factor of 10 over conventional photon counting with repetitive spark sources. The high repetition rate and excellent reproducibility and stability of a synchronously pumped dye laser give this technique a precision and dynamic range (more than 10^4) superior to that obtainable by the other methods. Very low intensities can be used, e.g. 10^9–10^{11} photons per pulse compared with 10^{13}–10^{16} photons per pulse for the Nd glass–streak camera system. For these reasons the photon counting technique is preferred for fluorescence measurements when the lifetime is greater than 100 ps.

As an example of the use of synchronously pumped dye laser – photon counting system and also because of its intrinsic interest in biochemical studies, we describe a study of the time resolved fluorescence of tryptophan and simple peptides related to it.

Fluorescence of tryptophan

The fluorescence from tryptophan in proteins is well known and has been extensively studied by both steady-state and time-resolved fluorescence spectroscopy. In the protein lysozyme, for instance, the multiple components in the tryptophan fluorescence decay have been assigned to emission from two of the six tryptophans, these having differing environments (Formoso & Forster 1975) and hence lifetimes. Even in a small single tryptophan-containing protein such as glucagon, as well as in tryptophan and a number of small peptides in solution, the fluorescence from the indole moiety decays non-exponentially. To understand the processes giving rise to this effect we have studied the fluorescence decays of glucagon, tryptophan, tryptophylalanine, alanyltryptophan and the parent compound, 3-methylindole, as a function of pH in aqueous solution. We have used the photon counting technique described below.

Experimental methods

Tryptophan, 3-methylindole, tryptophylalanine, alanyltryptophan and glucagon were obtained from Sigma and used without further purification. Samples were prepared in Analar water immediately before use and the appropriate pH obtained by using HCl (pH 1–3), commercial B.D.H. buffer tablets (pH 7 or 9.2) or NaOH (pH 11–13). The purity of the samples was checked by a comparison of the absorption, emission and excitation spectra as described in more detail below.

Absorption spectra were recorded on a Perkin-Elmer Hitachi 200 spectrometer with 1 nm resolution. The uncorrected fluorescence emission and excitation spectra were recorded on a Perkin-Elmer MPF-4 spectrofluorimeter. Steady-state irradiation of tryptophan samples was performed with the 254 nm line of a low pressure mercury lamp (*ca.* 10^{18} photons s^{-1}).

The fluorescence lifetimes were measured by using the single-photon counting apparatus shown in figure 1 and briefly described below. The extended cavity jet-stream dye laser

PHILOSOPHICAL TRANSACTIONS OF THE ROYAL SOCIETY A MATHEMATICAL, PHYSICAL & ENGINEERING SCIENCES

(Coherent Radiation CR 590) is synchronously pumped by the 514.5 nm line of an acousto-optically mode-locked argon ion laser. Under normal operating conditions the Ar^+ laser produces a highly stable train of *ca.* 90 ps pulses at a repetition frequency of 75.525 MHz; the average mode-locked power is *ca.* 800 mW. Synchronous mode-locking of the dye laser is achieved by extending the cavity to match that of the pump laser. With Rhodamine 6G as the lasing dye, a three-plate birefringent tuning element and a 30% output coupler, the average laser power is 200 mW at 590 nm. The laser pulse duration was determined from the second-order autocorrelation function measured by a zero-background second harmonic generation technique (Ippen & Shank 1975) and found to be 5 ps under these conditions.

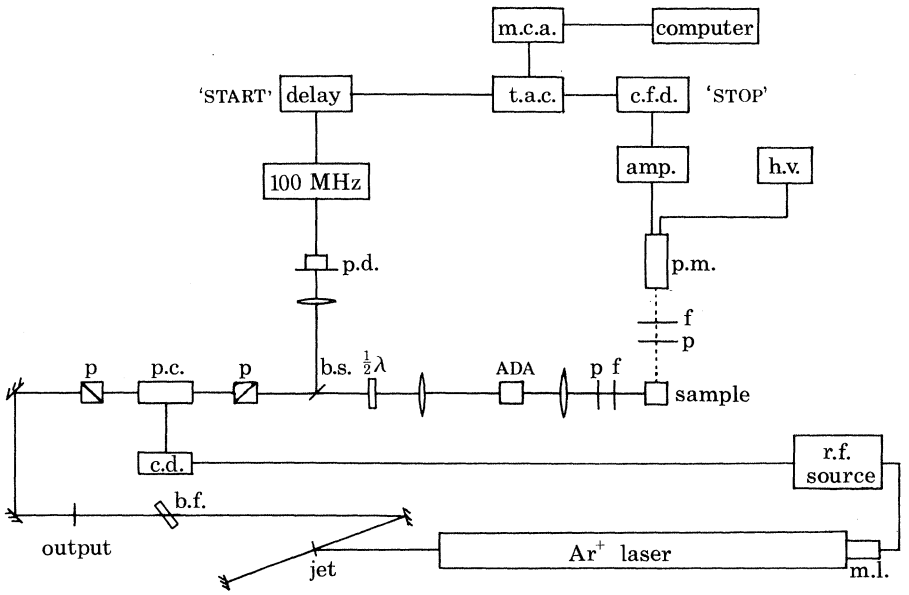

FIGURE 1. Block diagram of the synchronously pumped dye laser and photon counting instrument. Abbreviations: p, polarizers; p.c. Pockels cell; ADA, frequency doubling crystal; b.f., birefringent tuning element in the jet stream dye laser; f, filters; c.f.d., constant fraction discriminator; t.a.c., time–amplitude converter; p.d. photodiode.

The high repetition frequency of the dye laser output (75.5 MHz) introduces the danger of incomplete sample recovery between laser pulses in systems where long-lived transients might be formed. This problem is minimized by reducing the dye laser repetition frequency to 73.8 kHz by means of an electro-optic shutter consisting of a low-voltage Pockels cell between a pair of crossed polarizers; the trigger signal is derived from a synchronous output from the mode-locker r.f. source with fast countdown logic. The contrast ratio between the transmitted and rejected pulses is more than 500:1 with an amplitude stability of $\pm 10\%$ for the transmitted pulses.

The second harmonic (295 nm, vertically polarized) is generated by focusing the dye laser output into an ADA crystal 1 mm in length. The residual 590 nm radiation is removed by a polarizer and a Schott UG 11 filter. Phase-matching at 295 nm is achieved by maintaining the ADA crystal at 36.0 ± 0.2 °C with an Electro-Optic Developments TC 15 temperature controller; the maximum conversion efficiency is *ca.* 1%. Taking into account the various losses along the optical path, the estimated energy of a single u.v. pulse at the sample is *ca.* 1 pJ (*ca.* 1.5×10^6 photons).

A portion of the laser fundamental is diverted by a beam splitter and focused onto a Texas Instruments TIED 56 silicon avalanche photodiode. The diode output is used to trigger an Ortec model 436 100 MHz discriminator whose output is delayed by several nanoseconds in an Ortec model 425 time delay and serves as a 'START' signal for the Ortec model 457 time–amplitude converter (t.a.c.). The sample is placed in a 1 cm path length quartz cuvette and repetitively excited by the laser pulses. Fluorescence emitted at right angles to the excitation beam is isolated by appropriate filters and a polarizer and detected by a Mullard XP2020Q photomultiplier. To obtain the best time response in the single-photon counting application, the standard voltage divider network was modified in a manner similar to that described by Lewis *et al.* (1973). The single-photon anode pulses (*ca.* 100–400 mV into 50 Ω) are amplified in a Marconi model TF 2175 broadband amplifier (gain 27 ± 1 dB from 2–500 MHz) and fed into an Ortec model 463 constant fraction discriminator, and its output used as a 'STOP' signal for the time–amplitude converter. To eliminate 'pile-up', the excitation beam is attenuated so that the ratio of STOP to START pulses is always less than 2 %. The t.a.c. outputs are processed in a Tracor-Northern model TN-1706 multichannel analyser (m.c.a.), which is interfaced to an Interdata 7/32 computer.

The time calibration of the t.a.c.–m.c.a. combination is determined by spoiling the contrast ratio of the pulse selector and observing the channel separation of successive laser pulses scattered from a dilute suspension of talc. The time interval between the laser pulses (13.241 ns) is accurately defined by the frequency of the mode-locker r.f. source. The cables of the Ortec model 425 time delay are calibrated from this measurement and used to calibrate other ranges of the t.a.c. The absolute accuracy of the calibration procedure is estimated to be about 1 %.

In the measurement of short lifetimes by the single-photon technique, the fluorescence decay profile, $f(t)$, is obtained as the convolution of the true excited state decay function, $g(t)$, with the instrument response function $i(t)$:

$$f(t) = \int_0^t i(t-t')\, g(t')\mathrm{d}t'. \tag{1}$$

The fluorescence decay profile $f(t)$ is collected by exciting the sample at 295 nm and monitoring the resultant emission by using appropriate filters (Schott WG320, Balzer 340 nm interference or Schott GG400 filter) in front of the photomultiplier to remove scattered laser light. Polarization bias due to molecular rotation is eliminated by exciting with vertically polarized light and using an analyser (Polaroid HNP'B) orientated at 54.7 ° to the vertical (Knight & Selinger 1971). The instrument response function $i(t)$ is obtained by replacing the fluorescence sample with a dilute suspension of talc, removing the filter and collecting the scattered laser. radiation. In general, both the scattering and fluorescent samples have an absorbance of *ca.* 0.1 at 295 nm and the same decay profiles. Under normal operating conditions the instrument response function has a full width at half maximum of 360 ps.

We have chosen to extract the true fluorescence decay profile $g(t)$ from the experimental data by the iterative convolution technique. The strategy is to assume a functional form for $g(t)$, usually a sum of exponentials, and to adjust the values of the parameters until the 'best fit' is obtained between the experimental and calculated decay functions. The generally preferred procedure for obtaining the decay parameters is the method of least squares (Grinvald 1976). Computations for the nonlinear least-squares adjustment are performed on an Interdata 7/32 computer with a modified version of the Marquardt algorithm (Bevington 1969). Initially $g(t)$ is assumed to be of the form

$$g(t) = A\mathrm{e}^{-t/\tau}, \tag{2}$$

where A is the pre-exponential factor and τ is the fluorescence lifetime. The quality of the fit is judged from the reduced χ^2 criterion and by visual inspection of the weighted residuals (see figure 2). In those cases where a single exponential decay law is inadequate, a sum of exponentials is used:

$$g(t) = A\{f\mathrm{e}^{-t/\tau_1} + (1-f)\,\mathrm{e}^{-t/\tau_2}\} \tag{3}$$

where τ_1 and τ_2 are the lifetimes of the two components and f is the relative weight of the shorter component ($\tau_1 < \tau_2$). No attempts have been made to fit the data to more complex functions.

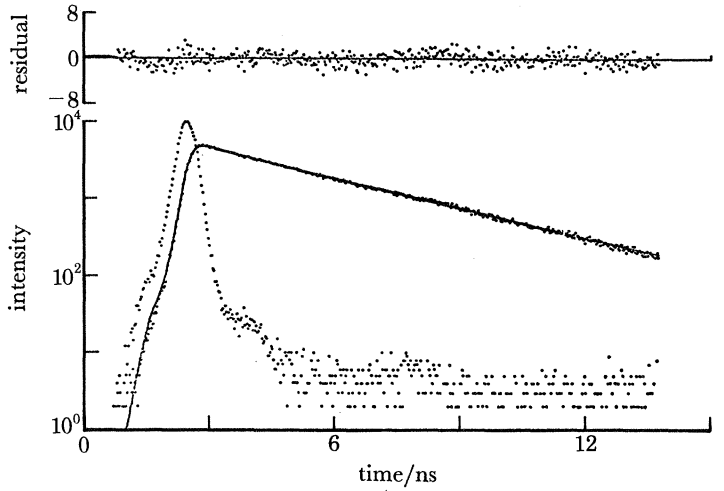

FIGURE 2. Fluorescence decay for aqueous tryptophan at pH 7, plotted on a log–linear scale. The solid line is the fitted curve to the fluorescence data (as points) after convolution with the measured instrument response function as shown as points. The residuals plot is shown at the top. See table 2 for lifetimes.

The response of photomultiplier tubes used in photon counting is known to depend on the wavelength of the light impinging on the photocathode (Lewis *et al.* 1973). Therefore the instrument response function collected at 295 nm by the scattering technique will not be an exact representation of the response function $i(t)$ required in (1) for deconvoluting fluorescence measurements made at longer wavelengths. Fortunately the wavelength dependence of the XP 2020 tube is very small; there is a delay of *ca.* 1 ps/nm with increasing emission wavelength, which is accompanied by small changes in the shape of the response function. The time shift of 50–60 ps is accounted for in the data analysis procedure by replacing $i(t)$ in (1) with $i(t-s)$, where s is a time-shift parameter. The change in shape is reflected by small systematic deviations on the rising edge of the decay curve. Even for the shortest lifetimes reported below, the errors are negligible.

GLUCAGON

In glucagon, which has 29 amino acid residues with tryptophan at position 25, the fluorescence from the tryptophan decays non-exponentially at 18 °C over the pH range 3–11. The structure (X-ray analysis), and molecular conformation in water, of this hormone have been extensively studied (Panjpan & Gratzer 1974); in dilute solution, glucagon adopts a flexible structure that exists as an equilibrium population of random coil conformers (Gratzer & Beavan 1969). At pH 11 there is a tendency to form an α-helical conformation in which the

non-polar residues 6–14 and 22–27 cluster together in two surface regions (Sasaki *et al.* 1975). These α-helices stabilize by forming trimers as a result of contact between the non-polar regions so that the hydrophobic residues are effectively buried (Sasaki *et al.* 1975).

In table 1 are shown data from some preliminary experiments on glucagon. It is clear that at each pH the decay is not exponential and that the decay times are invariant under these conditions. At pH 7 our values disagree with those of Conti & Forster (1975), who measured a single decay time of 3.1 ns (at pH 8.2), but agree well with the result of Grinvald & Steinberg (1976), who measured lifetimes of 1.1 and 3.6 ns.

Table 1. The pH dependence of the fluorescence lifetime of glucagon

pH†	τ_1/ns‡	τ_2/ns‡	f§	$\langle\tau\rangle$/ns‡
3‖	1.1_5	3.3	0.40	2.4
7‖	1.1_3	3.7	0.36	2.7_4
11‖	1.2_3	3.5	0.33	2.7_6
11¶	1.0_6	3.7	0.36	2.7_8

† All measurements in aqueous solution at 18 ± 1 °C.
‡ Estimated accuracy ± 5 %.
§ Estimated accuracy ± 0.03.
‖ Concentration *ca.* 0.2 mg/ml.
¶ Concentration *ca.* 2 mg/ml.

The population of trimers of the α-helical forms can be increased by about 20 times to 40 % at pH 11 by increasing the concentration from 0.2 mg/ml to 2 mg/ml. The two results at pH 11 are essentially the same despite the changes in conformation and degree of association occurring in the glucagon. This implies that the non-exponential decay is not due to the presence of multiple conformers and that the local environment of the tryptophan residue is not affected by conformational changes or molecular associations but is an intrinsic property of the tryptophan itself.

Tryptophan and 3-methylindole

Recently Rayner & Szabo (1978) examined the fluorescence decay of aqueous tryptophan by using conventional photon counting. The fluorescence was shown to be bi-exponential, with components of 3.14 and 0.5 ns which they attributed to the solvent equilibrated states ^1L_a and ^1L_b respectively. Fleming *et al.* (1978) have also reported non-exponential fluorescence decays of 2.1 and 5.4 ns duration in neutral solution.

The pH dependence of the fluorescence decay of tryptophan in aqueous solution has been studied over the pH range 1–13. Except at pH 11 the fluorescence decay is definitely not exponential, but can be fitted as a sum of two exponentials; by contrast, 3-methylindole decays exponentially over the whole pH range studied. In figure 2 are shown the fluorescence data obtained from tryptophan. The narrow curve is the instrument response function, the other points are the fluorescence, and the solid line is the computed fit to the fluorescence according to (3). This bi-exponential fit gives $\chi^2 = 1.07$ and lifetimes from ten such experiments gave lifetimes of 0.43 ± 0.2 ns, 3.32 ± 0.12 ns with 19 % of the shorter component present. A single exponential fit to the data yields a lifetime of 3.25 ns and a χ^2 of 1.7. The lifetime of 3-methylindole is 8.9 ± 0.13 ns over the pH range 3–11. The tryptophan lifetimes are in agreement with those of Rayner & Szabo (1978) but are in disagreement with those of Fleming *et al.* (1978). We have found that the long component in the decay observed by Fleming *et al.* can be obtained by

irradiating solutions with a low-pressure Hg lamp or by leaving the samples in the dark until bacterial action has begun. The decays obtained can be analysed into two components of 2.7 and 5.3 ns duration, although the decay is more complex than two exponentials. The agreement between these results and those obtained by using a Nd laser and streak camera (Fleming *et al.* 1978) suggests that photo-oxidation products may have accumulated during the 15 Nd laser shots required on each sample.

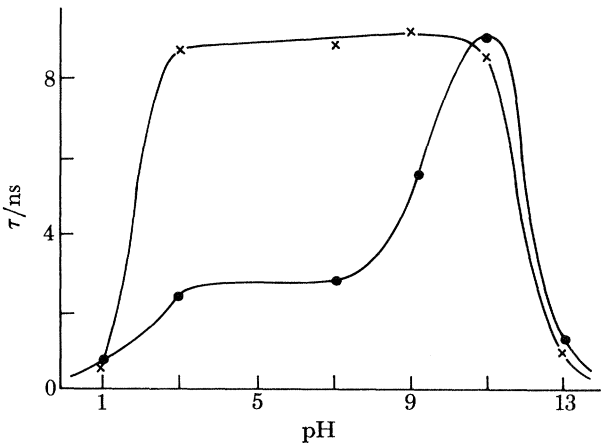

FIGURE 3. Fluorescence lifetime (nanoseconds) of 3-methylindole (×) and mean lifetime (where applicable) of tryptophan (●) plotted against pH.

TABLE 2. THE pH DEPENDENCE OF THE FLUORESCENCE LIFETIMES OF 3-METHYLINDOLE AND TRYPTOPHAN

3-methylindole		tryptophan			
pH†	τ/ns‡	τ_1/ns§	τ_2/ns‡	f‖	$\langle\tau\rangle$/ns§
1	0.77	0.29	0.80	0.27	0.66
3	8.7	0.29	3.0	0.23	2.4
7	8.9	0.43	3.3	0.19	2.8
9.2	9.3	3.0	9.0	0.56	5.6
11	8.5	¶	9.1	—	9.1
13	0.84	¶	1.2_1	—	1.2

† All measurements in aqueous solution at 18 ± 1 °C.
‡ Estimated accuracy ± 3 %.
§ Estimated accuracy ± 0.2 ns.
‖ Estimated accuracy ± 0.03.
¶ Single exponential.

In table 2 and figure 3 the lifetime data for 3-methylindole and tryptophan at 18 ± 1 °C are presented. In the figure the curve for tryptophan is obtained by plotting the mean lifetime, $\langle\tau\rangle = f\tau_2 + (1-f)\,\tau_2$.

At pH > 11 the lifetime of tryptophan is exponential and follows closely the behaviour of 3-methylindole, decreasing with an apparent $pK_a \approx 12$. In acid solutions the lifetimes of both compounds decrease to 1 ns but in the pH region 3–8 the tryptophan lifetime is not exponential and is greatly quenched from the value for 3-methylindole.

(*a*) *High* pH *region* (pH 11)

The fluorescence quenching of indole derivatives in alkaline solution was first observed by White (1959) and was attributed to an excited state proton transfer from the protonated nitrogen, thus producing the indole anion. This occurs with an apparent $pK_a \approx 12$. As the excited state equilibrium between indole and its anion is not established and as no anion fluorescence is obtained (neither are any additional transients observed in flash photolysis experiments), this proton transfer reaction must involve direct deactivation of the S_1 state to give the anion ground state. The rate for this deprotonation, calculated from our data, is a near diffusion controlled rate of 1.1×10^{10} l m^{-1} s^{-1}.

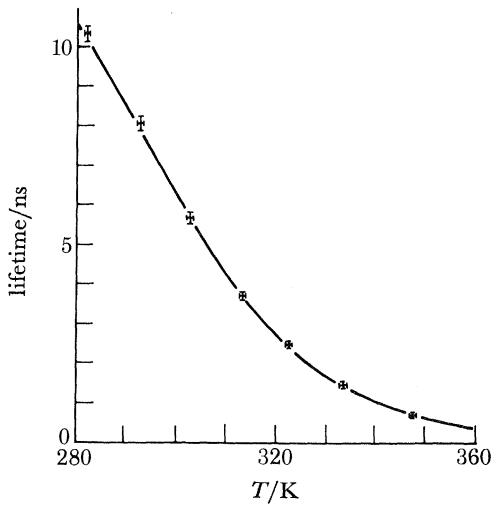

FIGURE 4. Fluorescence lifetime (nanoseconds) of 3-methylindole plotted against temperature (kelvins). The solid line is a fit to the data by using the equation $\tau^{-1} = k_0 + Ae^{-E/RT}$.

Photoionization has for some time been recognized as a possible non-radiative pathway for indole derivatives in solution (Baugher & Grossweiner 1977). The primary process appears to be an electron ejection leaving a radical cation, which can then deprotonate to a neutral radical. The indentity of the excited state precursor to photoionization has remained obscure. Bent & Hayon (1975) concluded from nanosecond flash photolysis that photoionization occurs from a vibrationally excited or higher excited singlet state, i.e. a pre-fluorescent state. The similar dependence of fluorescence triplet radical and electron yields suggest, however, that photoionization competes with the other processes in the S_1 state (Feitelson 1971; Grabner *et al.* 1977). According to the latter picture, the S_1 lifetime of 3-methylindole from pH 3–11 is governed by the rates of fluorescence k_f, intersystem crossing k_T and photoionization, k_{e^-}, i.e.

$$\tau^{-1}_{\mathrm{pH}\,11} = k_f + k_T + k_{e^-}.$$

At pH 11 the fluorescence lifetime of 3-methylindole decreases rapidly as the temperature is raised from 10 to 75 °C. It is generally accepted that for many indole derivatives both the rates of radiative and intersystem crossing processes are temperature insensitive over this range (Kirby & Steiner 1970). The observed decrease is then attributed to variations in the photoionization rate. At temperature T the measured fluorescence rate can be described by the equation

$$\tau^{-1} = k_0 + Ae^{-E/RT},$$

where $k_0 = k_f + k_T$, E is the activation energy for photoionization and A its 'frequency factor'. A least-squares analysis of the data, with the use of (4), yields $k_0 = 7.5 \pm 0.8 \times 10^7\ s^{-1}$; $A = 4 \times 10^{16}\ s^{-1}$; $E = 50 \pm 3$ kJ mol^{-1}. The data and the fitted curve are shown in figure 4. The values for k_0 and E are close to those obtained by other methods; $8.3 \pm 1 \times 10^7\ s^{-1}$ and 54 ± 6 kJ mol^{-1}, respectively (Kirby & Steiner 1970). At pH 11 the values for tryptophan are very similar: $E = 51 \pm 3$ kJ mol^{-1}, $k_0 = 8.3 \pm 0.6 \times 10^7\ s^{-1}$ and $A = 5 \pm 4 \times 10^{16}\ s^{-1}$.

We conclude from these experiments that as the amino group on the tryptophan exists as $-NH_2$ rather than as $-NH_3^+$ at neutral pH, the state of protonation of the side-chain amino group has no effect on the radiative decay rate of the indole chromophore.

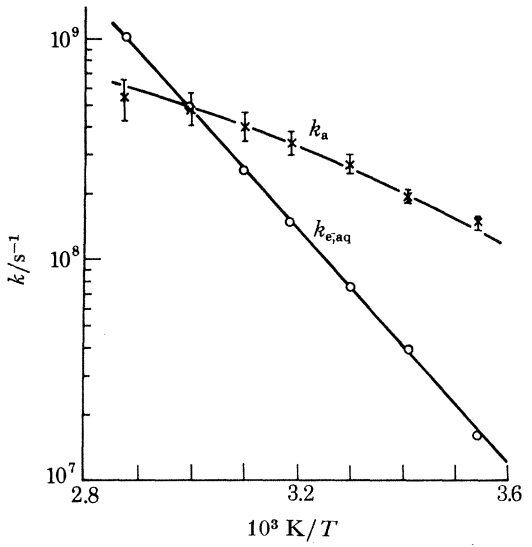

FIGURE 5. Photoionization rate ($k_{e^-,aq}$) plotted against reciprocal temperature for tryptophan. Experimental values (○), solid line represents a fit by using the equation $\tau^{-1} = k_0 + Ae^{-E/RT}$. Intramolecular quenching process (k_a) plotted against reciprocal temperature (×). Solid line is a fit by using the equation $K_a = Bt/\eta$.

(*b*) *Intermediate* pH *region* (pH 3–8)

According to our model, in the pH range 3–8 the additional quenching present in tryptophan over that in 3-methylindole is due to the interaction of the side chain with the ring rather than a change in the other processes. The measured fluorescence rate can be written as

$$\tau^{-1} = k_f + k_T + k_{e^-} + k_a = \tau_{pH\,11}^{-1} + k_a, \qquad (5)$$

where k_a is the rate of the intramolecular process. In this model we have explicitly assumed that we can transfer the rates k_f, k_T, k_{e^-} from pH 11 to pH 7.

The temperature dependence of the tryptophan lifetime at pH 7 was also analysed according to (4) and an apparent activation energy of 30 kJ mol^{-1} was obtained. The data at pH 11 suggest that photoionization has an activation energy of 50 kJ mol^{-1}. This conflict may be resolved by proposing that the intramolecular quenching process is also temperature dependent. Using (5) we obtain an activation energy of 16 kJ mol^{-1} for k_a. In figure 5 the data from pH 11 are plotted as k_{e^-} against T^{-1} as points, and the solid line together with points for k_a against T^{-1}.

A careful examination of these data reveals a systematic curvature in the plot of k_a against T^{-1} in excess of that expected from the magnitude of the experimental errors. If the intramolecular quenching process is diffusion controlled, expressing k_a in the Arrhenius form may not be valid. In the steady state the rate of the diffusional process is expected to be of the form $k_a = BT/\eta$, where B is a constant of proportionality and η is the solvent viscosity. The solid line through the data for k_a in Figure 5 is the best fit to the experimental points calculated from this equation with $B = 6.8 \times 10^5$ cP K^{-1} s^{-1}.† There is now no systematic deviation between the experimental and calculated data points.

In the ground state there is a near random conformation of the tryptophan side chain around the chromophore. When the chromophore becomes excited, the side chain must diffuse into the correct conformation for quenching to occur. This will clearly depend both on the solvent viscosity and temperature. Additionally, as some fractions of the side chains are already in the correct quenching configuration, they quench more rapidly than the average and give rise to the observed non-exponential fluorescence decay. This process is more familiar in the kinetics of diffusion controlled *inter*molecular quenching and has been studied extensively both theoretically (Noyes 1961) and experimentally (Beddard *et al.* 1978). A time dependent quenching rate is predicted from a solution of Fick's second law, i.e.

$$k(t) = 4\pi R(Q)\{1 + R/\sqrt{(\pi Dt)}\},$$

where D is the diffusion constant, R is related to the encounter distance and (Q) is the quencher concentration. Taking $D \approx 5 \times 10^{-5}$ cm^2 s^{-1}, $R \approx 3$ Å‡ as reasonable guesses for the quenching of tryptophan by the α-NH_3^+ group in the side chain, the quenching rate falls to 10% of its initial value in 600 ps. While this equation is not strictly valid, it does predict diffusion controlled quenching that has an intrinsic time dependence of the correct magnitude to explain the experimentally observed non-exponentiality.

(c) *Mechanism of the intramolecular quenching process*

Two mechanisms for the intramolecular quenching process in tryptophan are possible: (1) charge transfer interaction in which the excited indole chromophore acts as an electron donor and either a proton from the $-NH_3^+$ group or the carbonyl act as an acceptor (Kirby & Steiner 1970); (2) proton transfer from the $-NH_3^+$ group to the indole ring (Weinryb & Steiner 1968).

A short-lived (*ca.* 45 ns) transient (T_1) observed by Bent & Hayon (1975) in flash photolysis studies of aqueous tryptophan has been assigned to a triplet state. It has a maximum yield in the pH range 3–7 and disappears both in acid and alkaline solution. This pH profile strongly suggests that it comes from the intramolecular quenching process. While its identity is uncertain, it does have a similar spectrum and lifetime to a protonated excited indole formed at pH 2 and may be a triplet state formed by intramolecular proton transfer from the $-NH_3^+$ group to the 2-position on the indole chromophore.

The large deuterium isotope effect on the fluorescence quantum yield in neutral aqueous tryptophan solution has been studied by several investigators (Stryer 1966; Kirby & Steiner 1970; Nakanishi & Tsuboi 1978) and reflects the average effect on all the rate processes. The rate of the intramolecular quenching can be calculated from the formula $k_a = k_f(\phi^{-1} - \phi_{ref}^{-1})$,

† 1 cP = 1 mPa s. ‡ 1 Å = 10^{-10} m = 10^{-1} nm.

PHILOSOPHICAL TRANSACTIONS OF THE ROYAL SOCIETY A MATHEMATICAL, PHYSICAL & ENGINEERING SCIENCES

where ϕ is the fluorescence quantum yield of the tryptophan at pH 7, and ϕ_{ref} (3-methylindole) is 0.34 in H_2O and 0.50 in D_2O at 25 °C (Kirby & Steiner 1970). The isotope effect is then measured as the ratio $r = k_a(H_2O)/k_a(D_2O)$. For tryptophan $r = 2.9$; for the related compound tryptamine, $r = 2.3$; but for indole-3-propionic acid r is only 1.1. In addition, a large r value for tryptamine T_1 transient is also observed, whereas this is absent in indole-3-propionic acid.

These observations provide strong evidence that the intramolecular quenching process in tryptophan is dominated by a proton transfer reaction from the $-NH_3^+$ to the 2-position on the indole. A possible mechanism is shown in formula 1 where a six-membered ring is an intermediate in the reaction.

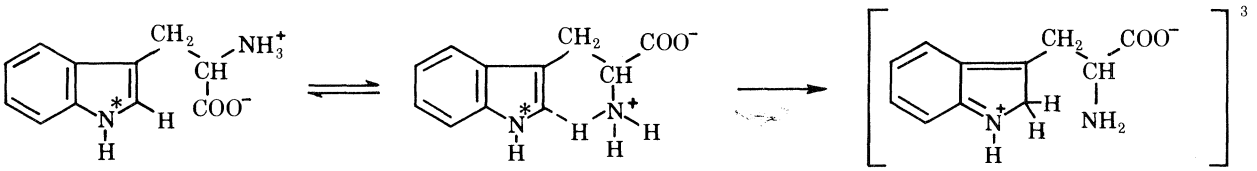

FORMULA 1

In the ester derivatives of indole-3-propionic acid, which contains no labile protons, a slight intramolecular quenching ability similar to that of the unionized acid is still present, excluding the possibility of a proton transfer mechanism. Cowgill (1963, 1967) has found a strong correlation between quenching efficiency and the electrophilicity of the carbonyl group in the series of compounds $-CO_2^- \approx -CONH_2 > COOH > COOEt$, and provides evidence for charge transfer quenching by the carbonyl group.

It thus appears that two intramolecular quenching mechanisms can operate on indole derivatives. When an $-NH_3^+$ group is in proximity to the indole ring, intramolecular proton transfer occurs and is characterized by a large deuterium effect and a T_1 transient. In derivatives without an $-NH_3^+$ group but possessing an electrophilic carbonyl, a charge transfer mechanism can occur.

(*d*) *Peptides containing single tryptophan residues*

We have also studied the pH dependence of the fluorescence lifetime of aqueous solutions of the simple peptides alanyltryptophan (Ala-Trp) and tryptophylalanine (Trp-Ala). Their structures are shown in formula 2. The fluorescence lifetimes of these compounds are shown in tables 3 and 4 and the pH profiles of the mean lifetimes plotted in figure 6. The fluorescence

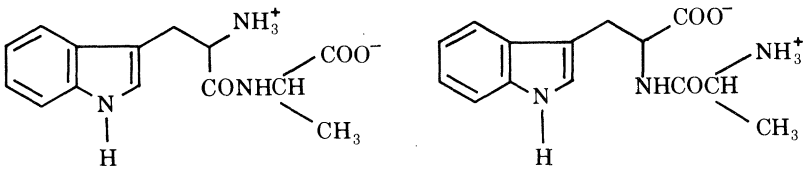

tryptophylalanine alanyltryptophan

FORMULA 2

properties of glycyltryptophan (Gly-Trp) and tryptophylglycine (Trp-Gly) at pH 7 have also been measured and, as with Ala-Trp and Trp-Ala, both are non-exponential. The lifetimes (at pH 7) are $t_1 = 0.58$, $t_2 = 1.55$, $f = 0.41$ for Gly-Trp, and $t_1 = 1.74$, $t_2 = 6.18$ and $f = 0.8$ for Trp-Gly, and are very similar to the values for the alanyl derivatives given in tables 3 and 4. This similarity enables us to make qualitative use of the previous work on glycyl derivatives in the interpretation of the Ala-Trp and Trp-Ala data. From the structure of Trp-Ala one may

expect the fluorescence properties to be similar to those of tryptophan and from figure 6 and table 2 one may see that this idea is approximately correct. As the $-NH_3^+$ in the side chain is deprotonated at high pH (above 9), the lifetime increases to a value close to that of 3-methylindole, becomes exponential and is quenched at high pH. In the pH range 3–7, Trp-Ala behaves like tryptophan, and a transient T_1 is observed. However, the deuterium isotope effect (r) is only 1.5 instead of 2.9 (with tryptophan), and is intermediate between a value for charge transfer (1.0) and proton transfer (2–3). Also, the lifetimes at each pH are a little lower than the corresponding values for tryptophan or 3-methylindole. In view of this shorter lifetime and the intermediate deuterium effect, it is possible that charge transfer quenching is also occurring so that in Trp-Ala and Trp-Gly both proton transfer and charge transfer mechanisms operate to shorten the lifetime.

TABLE 3. THE pH DEPENDENCE OF THE FLUORESCENCE LIFETIME OF TRYPTOPHYLALANINE

pH†	τ_1/ns‡	τ_2/ns‡	f§	$\langle\tau\rangle$/ns‡
1	0.24	0.97	0.31	0.74
3	0.47	1.9	0.38	1.4
7	1.6	5.9	0.68	2.9
9.2	‖	8.0	—	8.0
11	‖	7.5	—	7.5
13	‖	1.3_2	—	1.3_2

† All measurements in aqueous solution at 18 ± 1 °C.
‡ Estimated accuracy ± 5 %.
§ Estimated accuracy ± 0.03.
‖ Single exponential.

TABLE 4. THE pH DEPENDENCE OF THE FLUORESCENCE LIFETIME OF ALANYLTRYPTOPHAN

pH†	τ_1/ns‡	τ_2/ns‡	f§	$\langle\tau\rangle$/ns‡
1	0.17	0.58	0.26	0.47
3	0.41	1.2_2	0.49	0.82
7	0.73	2.0	0.48	1.4
9.2	0.65	3.0	0.22	2.4
11	0.68	2.9	0.19	2.5
13	0.92	1.9	0.96	0.96

† All measurements in aqueous solution at 18 ± 1 °C.
‡ Estimated accuracy ± 5 %.
§ Estimated accuracy ± 0.03.

In Ala-Trp the pH dependence of the fluorescence lifetime is again generally similar to that of tryptophan, but at each pH value the fluorescence is non-exponential and considerably quenched compared with tryptophan. These effects must be due to more efficient intramolecular quenching.

We have already noted that the carboxylate anion is not an efficient quencher, so the peptide group must be implicated as the quenching agent. In flash photolysis work on Gly-Trp no T_1 transient was observed and a deuterium effect of 1.08 was calculated, which means that no proton transfer quenching is present. The terminal $-NH_3^+$ group would appear to be too far away from the ring to allow an efficient proton transfer to occur in contrast with Trp-Ala or tryptophan.

PHILOSOPHICAL TRANSACTIONS OF THE ROYAL SOCIETY A MATHEMATICAL, PHYSICAL & ENGINEERING SCIENCES

The charge transfer interaction can be enhanced in Ala-Trp both by the presence of a slightly longer and hence more flexible side chain between the indole and the peptide carbonyl and by the the $-NH_3^+$ group's increasing the electrophilicity of the carbonyl by the inductive effect.

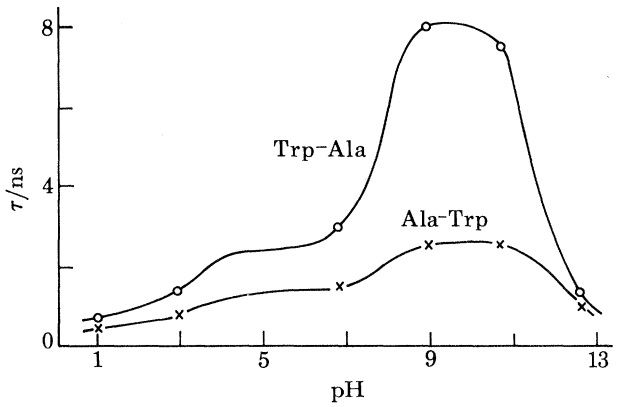

FIGURE 6. Mean fluorescence lifetimes (nanoseconds) for alanyltryptophan (×) and tryptophylalanine (○) plotted against pH.

CONCLUSION

In tryptophan and simple peptides, two quenching mechanisms operate. Then the $-NH_3^+$ group can form a six-membered ring by linking to the 2-position on the indole ring, and intramolecular proton transfer can occur with a higher probability than a charge transfer quenching. When the amino group is deprotonated, the interaction is removed and the compound behaves like 3-methylindole, i.e. the side chain is effectively absent and the fluorescence decays exponentially. When the amino group is absent or too far away for interactions as in Ala-Trp or Gly-Trp, charge transfer quenching between the peptide carbonyl and the ring occurs. When both $-NH_3^+$ and peptide carbonyl groups are present, as in Trp-Ala or Trp-Gly, both contribute to the quenching. In each case where the intramolecular quenching occurs, the fluorescence decay is not exponential and we believe that this arises from the initial non-random quenching positions of the side chains that are 'frozen in' as the molecule is excited.

We wish to thank the Science Research Council for overall support of this work. R.J.R. thanks the Royal Institution for a travel grant, and Dr R. Cooper for enabling him to spend an extended period in London. G.R.F. thanks the Leverhulme Trust Fund, and G.S.B. the Royal Society (John Jaffé Donation Research Fund), for the award of Fellowships.

REFERENCES (Beddard *et al.*)

Baugher, J. F. & Grossweiner, L. I. 1977 *J. phys. Chem.* **81**, 1349–1354.
Beddard, G. S., Carlin, S., Harris, L., Porter, G. & Tredwell, C. J. 1978 *Photochem. Photobiol.* **27**, 433–438.
Bent, D. V. & Hayon, E. 1975 *J. Am. chem. Soc.* **97**, 2612–2619.
Bevington, P. R. 1969 *Data reduction and error analysis for the physical sciences*. New York: McGraw-Hill.
Conti, C. & Forster, L. S. 1975 *Biochem. biophys. Res. Commun.* **65**, 1257–1263.
Cowgill, R. W. 1963 *Arch. Biochem. Biophys.* **100**, 36–44.
Cowgill, R. W. 1967 *Biochim. biophys. Acta* **133**, 6–18.
Feitelson, J. 1971 *Photochem. Photobiol.* **13**, 87–96.

PHILOSOPHICAL TRANSACTIONS OF THE ROYAL SOCIETY A MATHEMATICAL, PHYSICAL & ENGINEERING SCIENCES

Fleming, G. R., Morris, J. M., Robbins, R. J., Woolfe, G. J., Thistlethwaite, P. J. & Robinson, G. W. 1978 *Proc. natn. Acad. Sci. U.S.A.* **75**, 4652–4656.
Formoso, C. & Forster, L. S. 1975 *J. biol. Chem.* **250**, 3738–3745.
Grabner, G., Kohler, G., Zechner, J. & Getoff, N. 1977 *Photochem. Photobiol*, **26**, 449–458.
Gratzer, W. B. & Beavan, G. H. 1969 *J. biol. Chem.* **244**, 6675–6679.
Grinvald, A. 1976 *Analyt. Biochem.* **75**, 260–280.
Grinvald, A. & Steinberg, I. Z. 1976 *Biochim. biophys. Acta* **427**, 663–678.
Ippen, E. P. & Shank, C. V. 1975 *Appl. Phys. Lett.* **27**, 488–490.
Kirby, E. P. & Steiner, R. F. 1970 *J. phys. Chem.* **74**, 4480–4490.
Knight, A. E. W. & Selinger, B. K. 1971 *Spectrochim. Acta* A **27**, 1223–1234.
Lewis, C., Ware, W. R., Doemeny, L. J. & Nemzek, T. L. 1973 *Rev. scient. Instrum.* **44**, 107–114.
Nakanishi, M. & Tsuboi, M. 1978 *Chem. Phys. Lett.* **57**, 262–264.
Noyes, R. M. 1961 *Prog. React. Kinet.* **1**, 129–160.
Panjpan, B. & Gratzer, W. B. 1974 *Eur. J. Biochem.* **45**, 547–553.
Porter, G., Tredwell, C., Searle, G. & Barber, J. 1978 *Biochim. biophys. Acta* **501**, 232–245.
Rayner, D. M. & Szabo, A. G. 1978 *Can. J. Chem.* **56**, 743–745.
Sasaki, K., Dockerill, S., Adamiak, D. A., Tickle, I. J. & Blundell, T. 1975 *Nature, Lond.* **257**, 751–757.
Searle, G., Barber, J., Porter, G. & Tredwell, C. 1978 *Biochim. biophys. Acta* **501**, 246–256.
Stryer, L. 1966 *J. Am. chem. Soc.* **88**, 5708–5712.
Weinryb, I. & Steiner, R. F. 1968 *Biochemistry N.Y.* **7**, 2488–2495.
White, A. 1959 *Biochem. J.* **71**, 217–220.

PHILOSOPHICAL TRANSACTIONS OF THE ROYAL SOCIETY A MATHEMATICAL, PHYSICAL & ENGINEERING SCIENCES